Oxygen-proof fluorescence temperature sensing with pristine C_{70} encapsulated in polymer nanoparticles†

Vera Augusto, Carlos Baleizão,* Mário N. Berberan-Santos and José Paulo S. Farinha*

Received 6th October 2009, Accepted 5th November 2009
First published as an Advance Article on the web 16th December 2009
DOI: 10.1039/b920673f

We report the first successful encapsulation of pristine fullerene C_{70} in polymer nanoparticles with very low size polydispersity. We obtained water-dispersed polystyrene (PS) nanoparticles with diameters from 60 nm to 190 nm using a miniemulsion polymerization technique. Contrarily to pristine fullerenes, which are insoluble in most solvents and materials, the nanoparticles containing fullerene C_{70} (PS-C_{70}) are stable in water and can be easily incorporated in different materials. When blended with polyacrylonitrile (PAN), a virtually oxygen-impermeable polymer, the PS-C_{70} nanoparticles show a strong temperature dependence of the thermally activated delayed fluorescence (TADF) intensity and lifetimes, even when exposed to air. This is the first fluorescence temperature sensor based on TADF that can operate in the presence of oxygen. Unlike other fluorescence temperature sensors, our sensor material is insensitive to oxygen, has emission lifetimes in the millisecond range, and shows a strong emission intensity increase when the temperature increases. This sensor exhibits a very broad sensitivity in a working range from −75 °C to at least 105 °C (based on fluorescence intensity), surpassing the performance of other temperature fluorescence sensors at high temperatures.

Introduction

Since their discovery and production in macroscopic amounts,[1,2] fullerenes have attracted increasing attention because of their application in materials for energy, electronics, optics, biology, *etc*.[3] Pristine fullerenes (C_{60}, C_{70}, C_{76}, and higher fullerenes) are only moderately soluble in a few solvents, mostly aliphatic and aromatic hydrocarbons.[4] Although fullerene derivatives can have higher solubility than the pristine compounds, in either hydrophobic or hydrophilic solvents, their photophysical properties are often very different. For example, C_{70} adducts do not show the strong temperature and oxygen concentration-dependent Thermally Activated Delayed Fluorescence (TADF) emission of the pristine compound, and are therefore unsuited for applications as oxygen- and temperature-sensors.[5] This solubility issue is therefore a major drawback for the applications of unfunctionalized fullerenes. Some attempts have been made previously to encapsulate pristine fullerenes into different materials, such as micelles,[6] inorganic mesoporous materials and zeolites,[7] sol-gel based materials,[8] and polymers. In all cases, the obtained materials showed low stability and poor versatility, either requiring severe synthetic conditions, and/or leading to fullerene aggregation. Blending of pristine fullerenes in polymer films[9] is also restricted to a very limited number of cases where the fullerene is soluble in the polymer and a good solvent for both is available. Until now, there has been no easy, versatile and useful strategy to incorporate pristine fullerenes in different materials.

One way to increase the variety of materials where pristine fullerenes can be incorporated without aggregation is to encapsulate the fullerenes in polymer nanoparticles. The particles can then be incorporated in the desired materials, performing surface modification if needed. So far, this has only been accomplished for fullerene derivatives,[10] which can either be covalently linked to the polymer, or have their solubility tailored for better mixing with the growing polymer chains during polymerization. The use of fullerene derivatives has many disadvantages though. Not only is their synthesis relatively complex and has low yields, but their properties are often less desirable than those of the pristine fullerenes.

The incorporation of unmodified fullerenes in polymer nanoparticles by emulsion polymerization processes is not viable due to their insolubility in water. However, by using miniemulsion polymerization[11] we could obtain fullerene-loaded monodisperse and kinetically stable monomer droplets. In contrast to conventional emulsion systems, the small size of the monomer droplets in the miniemulsion provides a large surface area for radical capture, so that polymerization of the droplets yields the desired fullerene-loaded polymer nanoparticles of uniform size. The miniemulsion process also allows the specific modification of the particle surface by inserting functional groups, which can be used to incorporate the particles in different materials, to covalently bind biomolecules to their surface, *etc*.

One of the most characteristic and interesting photophysical properties of C_{60}, C_{70}, and some of their derivatives is a second mechanism of fluorescence, called *thermally activated delayed fluorescence* (TADF).[12] The TADF mechanism, which is a relatively uncommon phenomenon, takes place after excitation and intersystem crossing (ISC) from the first excited singlet state S_1 to

CQFM-Centro de Química-Física Molecular and IN-Institute of Nanoscience and Nanotechnology, Instituto Superior Técnico, 1049-001 Lisboa, Portugal. E-mail: carlos.baleizao@ist.utl.pt; farinha@ist.utl.pt; Fax: +351 218464455; Tel: +351 218419221

† Electronic supplementary information (ESI) available: Quantum yield of triplet formation and S_1-T_1 energy gap of PS-C_{70}. See DOI: 10.1039/b920673f

the triplet manifold (T_1 or a higher triplet), followed by a second ISC from T_1 back to S_1, and fluorescence emission. The unmodified fullerene C_{70} displays an outstanding TADF emission, and although other fullerenes (C_{60}, C_{60} derivatives, and one C_{70} derivative) and other molecules (xanthene dyes, aromatic ketones and thiones, metal porphyrins, and aromatic hydrocarbons) also exhibit TADF, this is much weaker than that of C_{70}.[5]

Recently, a fluorescence temperature sensor based on C_{70} dispersed in bulk polystyrene has been developed, taking advantage of the strong TADF exhibited by C_{70} in the absence of oxygen.[13] The sensitivity of TADF towards oxygen is very high, with 50 ppm of oxygen causing a 60% decrease in the fluorescence lifetime of C_{70}.[14] One strategy to obtain a sensor that can operate in the presence of oxygen is to encapsulate the fullerenes in an oxygen-impermeable material. Unfortunately, all attempts to directly incorporate C_{70} in these materials were unsuccessful due to the very low solubility of the fullerene, which leads to C_{70} aggregation and consequent quenching of the TADF.

In the work presented here we have solved this problem by encapsulating the pristine C_{70} in polymer nanoparticles that can subsequently be dispersed in an oxygen-impermeable material. We describe the encapsulation of unfunctionalized fullerene C_{70} in polystyrene (PS) nanoparticles of controlled diameter through miniemulsion polymerization. By dispersing the polystyrene nanoparticles containing C_{70} (PS-C_{70}) in polyacrylonitrile (PAN) (a virtually oxygen-impermeable polymer) we obtained a material that can be used as a fluorescence temperature sensor in the presence of oxygen, thus avoiding the use of vacuum or an oxygen-free atmosphere. This opens opportunities for application in areas such as temperature-sensitive paints and coatings, medical diagnosis, *etc*.

Experimental

Materials

Styrene (99%, Aldrich) and divinylbenzene (DVB, 80%, Aldrich) were distilled before use. Hexadecane (99%, Aldrich), sodium dodecyl sulfate (SDS, 99%, Aldrich), potassium persulfate (KPS, 99.99%, Aldrich), sodium hydrogencarbonate ($NaHCO_3$, 99.7%, Aldrich), C_{70} (99%, Mer Corporation), and polyacrylonitrile (PAN, MW 150 000, Polysciences) were used as received.

Preparation of PS-C_{70} particles with 60 nm diameter

An aqueous solution of SDS (0.58 g) and $NaHCO_3$ (28 mg) in 53.33 g deionized water and an organic solution of styrene (18 g), C_{70} (93 mg, previously dissolved in the styrene), hexadecane (0.48 g) and DVB (91 mg) were magnetically stirred for 30 min. The resulting emulsion was then sonicated (Branson 250/450 digital sonifier, with 50% amplitude and 1 s pulse on/2 s pulse-off) in an ice bath for 60 s. The resulting miniemulsion was added to a three-necked 500 mL round-bottom reactor equipped with a condenser, mechanical stirrer and gas inlet. The mixture was stirred and degassed with argon for 30 min. The solution was then heated to 70 °C, and the KPS (0.136 g) in aqueous solution (1% of the water used in the synthesis) was poured into the reaction flask. The mixture was then allowed to react for 8 h under constant stirring, and finally cooled to room temperature.

Preparation of PS-C_{70} particles with 190 nm diameter

The procedure was similar to the previous section. The quantities used were: styrene (7.4 g), C_{70} (37 mg), hexadecane (40 mg), DVB (38 mg), SDS (51 mg), $NaHCO_3$ (0.28 g), deionized water (40 g), and KPS (44 mg). The emulsion was sonicated for 12 min.

Film preparation

All the films were prepared in a hydraulic heated press (Carver Inc mod. 3851-0) from freeze-dried particles, using 15 cm × 15 cm Mylar® masks (125 μm thick polyester foil, Goodfellow). The films of PS-C_{70} were prepared by applying a pressure of 178 ton/m^2 during one hour, at 120 °C. The films of PS-C_{70}/PAN were prepared from a mixture of 5 wt% PS-C_{70} freeze-dried nanoparticles with PAN, by applying 440 ton/m^2 during 2.5 hours at 140 °C.

Characterization

The solid content of the water-dispersed particles was obtained by gravimetric analysis. Hydrodynamic particle radii were obtained by dynamic light scattering (Brookhaven Instruments: BI-200SM goniometer, BI-APD avalanche photodiode detector and BI-9000AT autocorrelator; Spectra Physics He-Ne laser with 35 mW at 632.8 nm) of diluted particle dispersions in water (0.005 wt%). The autocorrelation functions were analyzed by Laplace inversion and by a sum of exponential functions (CONTIN and Expsam V3.0 programs, BI-ZP software package from Brookhaven). The absorption spectra were recorded using a Shimadzu UV-3101PC UV-Vis-NIR spectrophotometer and the fluorescence measurements were obtained using a Spex Fluorolog F112A fluorimeter using a front face configuration. Laser scanning confocal fluorescence microscopy (LSCFM) images were obtained using a Leica TCS SP5 laser scanning microscope using an HC PL APO CS 0.4 dry 50× objective.

Time-resolved picosecond fluorescence intensity decays were obtained by the single-photon timing method with laser excitation at 590 nm and emission at 700 nm. The set-up consists of a diode-pumped solid state Nd:YVO4 laser (Milennia Xs, Spectra Physics) that can synchronously pump a mode-locked Ti:Sapphire laser (Tsunami, Spectra Physics, with tuning range 700–1000 nm, output pulses of 100 fs, and 80 MHz repetition rate that can be reduced down to 4 MHz by a pulse picker) or a cavity-dumped dye laser (701-2, Coherent, delivering 3–4 ps pulses of *ca.* 40 nJ pulse^{-1} at 3.4 MHz) working with rhodamine 6G. Intensity decay measurements were made by alternated collection of impulse and decays with the emission polarizer set at the magic angle position. Impulses were recorded slightly away from the excitation wavelength with a scattering suspension. For the decays, a cut-off filter was used to effectively remove excitation light. Emission light was passed through a depolarizer before reaching the monochromator (Jobin-Yvon HR320 with a 100 lines/mm grating) and detected using a Hamamatsu 2809U-01 microchannel plate photomultiplier. No less than 10 000 counts were accumulated at the maximum channel. The decay curves were analyzed using a non-linear least-squares reconvolution method.[15]

Results and discussion

Synthesis of PS-C_{70} nanoparticles

A series of C_{70} containing PS nanoparticles (PS-C_{70}) of different diameters were synthesized by a miniemulsion polymerization procedure (Scheme 1a). The amount of C_{70} was controlled to obtain 0.5 wt% of C_{70} in the final particles – a value corresponding to the maximum solubility of C_{70} in styrene. The particles were cross-linked by adding 1% of divinylbenzene (DVB), except those used to test the reactivity of styrene towards C_{70} in miniemulsion conditions. The solid content of the dispersions at the end of the polymerization was of the order of 20–22% in all runs, indicating that the overall conversion of the styrene was around 100%. Almost no coagulum was observed after polymerization.

If the sonication of the mixture is enough for the droplets to reach a pseudo-steady state, the size of the final particles depends mainly on the surfactant to monomer ratio, which determines the surfactant coverage of the particles, and is almost insensitive to the amount of hydrophobic stabilizer.[16] In the present work, we prepared particles with diameters of 60 ± 2 nm and 190 ± 13 nm (measured by dynamic light scattering) and low size polydispersity (Fig. 1). TEM images of the polymer nanoparticles (Fig. 1) show that the particle diameters are very similar to those obtained from dynamic light scattering. Based on the quantities of C_{70} and styrene used in the synthesis, the particles with 60 nm and 190 nm diameter have an average of 500 and 1.6×10^4 C_{70} molecules per particle, respectively.

A water-soluble initiator (potassium persulfate, KPS) was used in the polymerization in order to reduce the probability of C_{70} reaction, previously described for bulk polymerization of styrene in the presence of C_{60} and C_{70}.[9,17] The yield of the bulk radical polymerization of styrene in the presence of C_{70} using AIBN as an initiator is only about 20%, and on average each polymer chain contained only one molecule of fullerene.[17b] In our case, this reaction is not expected to occur since the initiator is water-soluble and the polymerization of styrene yields approximately 100% conversion (gravimetric determination). In any case, the occurrence of this unwanted reaction in miniemulsion conditions was assessed using particles of 60 nm diameter synthesized without cross-linker. After the polymerization, the particles were freeze-dried and dissolved in toluene. Unlike the results obtained for the bulk polymerization of styrene with C_{70},[9,17] the fluorescence spectrum is very similar to that of pure C_{70} in the same solvent (Fig. 2). The fluorescence spectra of uncross-linked PS-C_{70} nanoparticles present the two characteristic maxima of pristine C_{70}. In fact, the fluorescence spectra of C_{70} is very sensitive to any kind of modification (the fluorescence spectra of adducts only presents one maximum at 685 nm).[18]

The room temperature prompt fluorescence lifetime decays of films cast from uncross-linked PS-C_{70} nanoparticles and C_{70} dispersed in bulk PS were also very similar, with no component corresponding to C_{70} adducts being observed. The fact that no emissive adducts of C_{70} are detected and the high conversion of styrene indicate that C_{70} does not react with the propagating

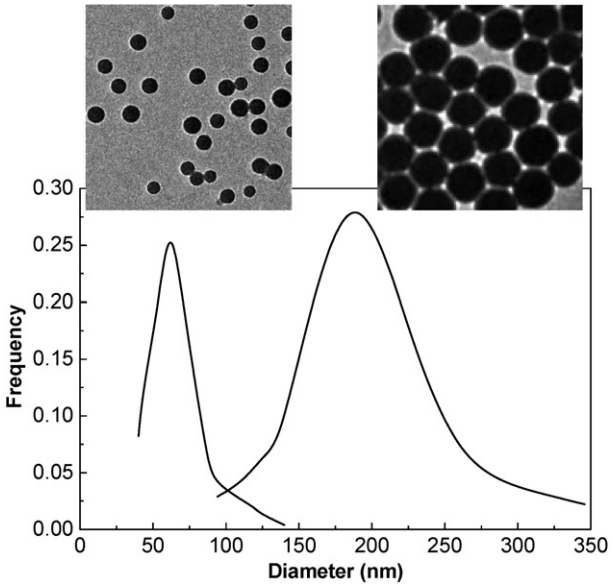

Fig. 1 Diameter distribution of PS-C_{70} particles with 60 ± 2 nm and 190 ± 13 nm (histogram obtained from several measurements by dynamic light scattering) and corresponding TEM images (1 μm × 1 μm).

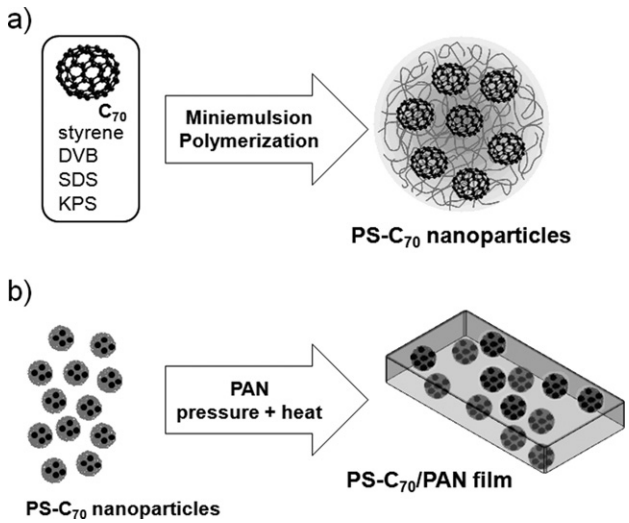

Scheme 1 (a) Encapsulation of C_{70} in PS nanoparticles through miniemulsion polymerization. (b) Blending of PS-C_{70} nanoparticles with PAN and film formation by applying pressure and heat.

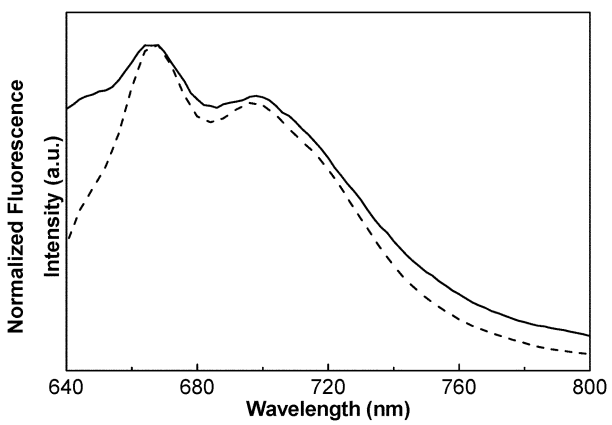

Fig. 2 The normalized fluorescence spectrum of uncross-linked PS-C_{70} nanoparticles dissolved in toluene (—) is very similar to the spectrum of C_{70} in toluene (---).

radicals during miniemulsion polymerization of styrene using KPS as initiator.

Fluorescence of PS-C_{70} nanoparticles

The C_{70}-containing PS nanoparticles (PS-C_{70}) were freeze-dried and cast into films. The absorption and fluorescence spectra, the prompt fluorescence lifetime ($\tau_F = 0.70$ ns) and the phosphorescence lifetime ($\tau_P = 48$ ms at 77 K) of the PS-C_{70} films in vacuum (10^{-5} mbar) were similar to those of C_{70} dispersed in bulk polystyrene under the same conditions.[13] These results indicate that the C_{70} is intact and molecularly dispersed inside the nanoparticles and that no detectable aggregation occurs.

The fluorescence intensity of degassed films prepared from PS-C_{70} particles increases with temperature due to the occurrence of TADF. Fig. 3 shows the fluorescence intensity measured between 20 °C and 90 °C. The effect of increasing/decreasing fluorescence intensity is completely reversible and after several heating–cooling cycles no hysteresis is observed. The high triplet quantum yield ($\Phi_T = 0.99$) and low singlet–triplet energy gap ($\Delta E_{ST} = 29$ kJ mol^{-1}) (ESI,† Fig. S1) are identical to the values for C_{70} directly dispersed in bulk PS and measured under vacuum.[13] The delayed fluorescence lifetime in the absence of oxygen at 20 °C is $\tau_{DF} = 27.2$ ms, and drops to $\tau_{DF} = 10.4$ ms at 90 °C. The PS-C_{70} films can be stored for months in the dark at room temperature, maintaining their photophysical characteristics. No influence of the nanoparticle diameter (60 and 190 nm) was observed on the photophysical properties.

PS-C_{70} nanoparticles in an oxygen-impermeable matrix

The main advantage of using C_{70} encapsulated in PS nanoparticles is that, unlike the pristine C_{70}, the particles can be incorporated in different materials. This can be done without affecting the properties of C_{70}, either by modifying the particle surface or by blending with other polymers.[19] In the present work, we demonstrate the incorporation of PS-C_{70} particles in polyacrylonitrile (PAN), a polymer where C_{70} itself is completely insoluble. PAN is often used as a matrix in temperature sensors to avoid oxygen interference by quenching [20] because it has an extremely low gas permeability ($P = 1.5 \times 10^{-17}$ cm^2 Pa s^{-1}).[21]

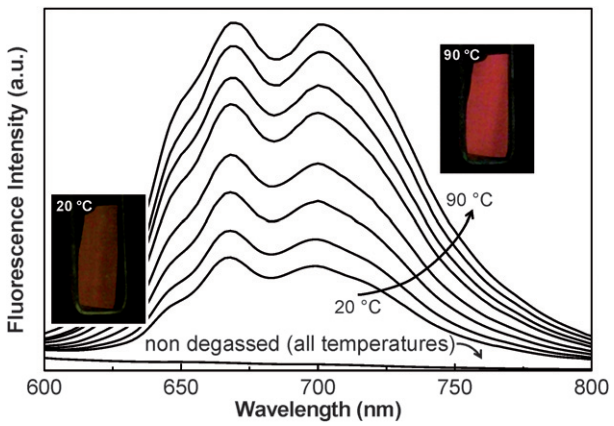

Fig. 3 Fluorescence spectra ($\lambda_{exc} = 470$ nm) of a degassed film of PS-C_{70} nanoparticles at different temperatures (20 °C to 90 °C in 10 °C steps). The emission of the non-degassed sample is also shown for comparison. The photos show the film under UV illumination at 20 °C and 90 °C.

We prepared 125 μm thick films containing 5 wt% PS-C_{70} nanoparticles in a PAN matrix (Scheme 1b) by pressure casting a mixture of the particles and PAN (440 ton/m^2 during 2.5 hours at 140 °C – a temperature above the glass transition temperature of both polymers). The film was examined by laser scanning confocal fluorescence microscopy to assess the compatibilization between the PS-C_{70} nanoparticles and the PAN (Fig. 4). The film exhibits some phase segregation between the two polymers (the dark areas in Fig. 4 are pure PAN domains), probably due to the thermal treatment. The aggregation of PS-C_{70} nanoparticles on the film does not affect the photophysical properties of the PS nanoparticles.

The fluorescence intensity of the PS-C_{70}/PAN films increases when the temperature is increased, even when the films are directly exposed to air (Fig. 5). This was the first observation of fullerene TADF in a material subject to atmospheric oxygen concentrations. The fluorescence intensity is completely reversible when heating–cooling cycles are performed, with no hysteresis being observed. Furthermore, the delayed fluorescence lifetimes (τ_{DF}) measured for the PS-C_{70}/PAN films exposed to air are similar to the lifetimes obtained for degassed PS-C_{70} films (Fig. 6). The observed strong temperature dependence, together with the long values of the lifetimes (in the millisecond range) in the presence of oxygen, makes the PS-C_{70}/PAN films excellent fluorescence temperature sensors.

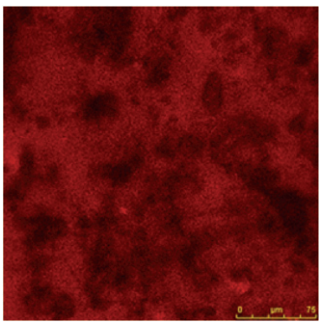

Fig. 4 Laser scanning confocal fluorescence image (150 μm × 150 μm) of a PS-C_{70}/PAN film obtained by blending 5 wt% PS-C_{70} dried nanoparticles with PAN and pressure casting at 440 ton/m^2 during 2.5 hours at 140 °C.

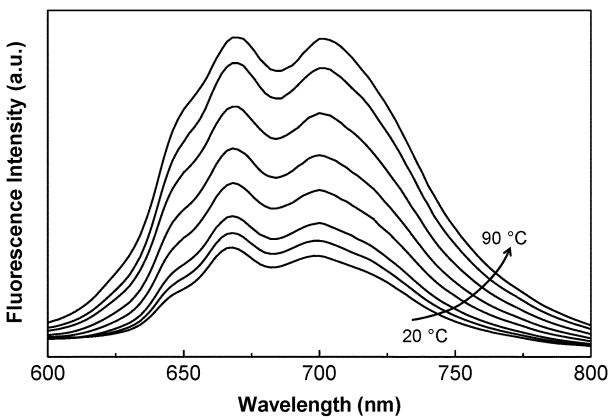

Fig. 5 Fluorescence spectra ($\lambda_{exc} = 470$ nm) of a PS-C_{70}/PAN film exposed to air at different temperatures (from 20 °C to 90 °C in 10 °C steps, corrected for light scattering).

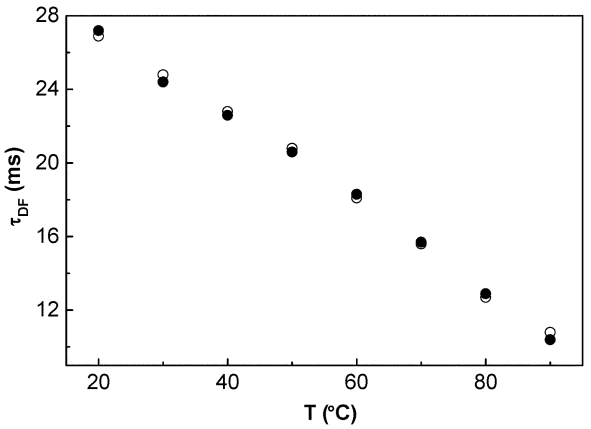

Fig. 6 Temperature dependence of the fluorescence lifetimes (τ_{DF}) of PS-C_{70} films in vacuum (●) and PS-C_{70}/PAN film exposed to air (○), with excitation at 470 nm and emission at 700 nm.

The PS-C_{70}/PAN films also preserve their photophysical properties after storage at room temperature for several months. The photostability of the PS-C_{70}/PAN sensor films was evaluated by measuring τ_{DF} after 8 h of continuous irradiation at 470 nm using a 150 W Xenon lamp. No change in the delayed fluorescence lifetime was observed, both at room temperature and at 70 °C.

PS-C_{70}/PAN sensor applicability

Luminescence based sensors are a versatile, well-established and efficient class of temperature sensors. The use of fiber optics in combination with phosphors for temperature sensing based on luminescence lifetime changes has been widely used.[22] More recently, a new class of optical sensors based on fluorescence and exploiting the temperature dependence of either intensity, or lifetime have been explored.[23] The use of fluorescence temperature based sensors in real applications is very simple because they can be easily incorporated in fiber optic sensor platforms[24] using simple available excitation sources like LEDs, and the signal can be collected in time or phase mode. Additionally, they exhibit a very fast response, they are reversible, and the spatial resolution can go from the macroscale (fluorescent paints) down to the nanoscale (fluorescence microscopy).[25]

Ruthenium(II) polypyridyl complexes, especially Ru(II) tris-(phenanthroline) ($Ru(phen)_3$),[20] are widely used as temperature probes because of their strong temperature luminescence dependence.[23a] The luminescence properties (intensity and lifetime) of these complexes when incorporated in an impermeable matrix (like PAN) display efficient thermal quenching and, consequently, high sensitivity.[20] Because of the quenching, these complexes have a lower performance for temperatures higher than 70–80 °C, for which the fluorescence intensity almost vanishes and the lifetime drops below 1 μs. Comparison of the performance of $Ru(phen)_3$ based sensors and our PS-C_{70} sensor should consider the fluorescence intensity and lifetime. As mentioned before, the fluorescence intensity of PS-C_{70} increases with temperature (Fig. 3), as opposed to that of $Ru(phen)_3$, and the lifetimes are in the millisecond range (Fig. 6), three orders of magnitude higher than those of $Ru(phen)_3$.[20] These two differences account for the higher temperature sensitivity of our new PS-C_{70}/PAN sensor, both regarding fluorescence intensity and lifetimes.

The temperature sensitivity of the fluorescence intensity can be measured by the relative sensitivity (S_R), which measures the variation of the fluorescence quantum yield (Φ_F) with temperature:

$$S_R = \frac{1}{\Phi_F}\frac{d\Phi_F}{dT} = \frac{d\ln\Phi_F}{dT} \quad (1)$$

The quantum yield reflects directly the variation of fluorescence intensity. In our case, the ratio between the delayed fluorescence intensity (I_{DF}) and the prompt fluorescence intensity (I_{PF}) for the different temperatures (Fig. 3) can be fitted using

$$\frac{I_{DF}}{I_{PF}} = \left[\frac{1}{\Phi_T} - 1 + \left(\frac{1}{\Phi_T}\left(\frac{1}{\Phi_S^{\infty}} - 1\right)\right)e^{\left(-\frac{\Delta E_{ST}}{RT}\right)}\right]^{-1} \quad (2)$$

where Φ_S^{∞} is the quantum yield of singlet formation at very high temperatures. The experimental and calculated values of I_{DF}/I_{PF} at 700 nm (Fig. 3), and the relative sensitivity S_R calculated from fluorescence intensity (eqn (1)) for PS-C_{70} nanoparticles are presented in Fig. 7A. A minimum value of $S_R = 0.5\%\ °C^{-1}$ was considered for practical usage, yielding a temperature working range from −75 °C to at least 105 °C. The Φ_F of PS-C_{70} increases with temperature, reaching a maximum value around 0.04. On

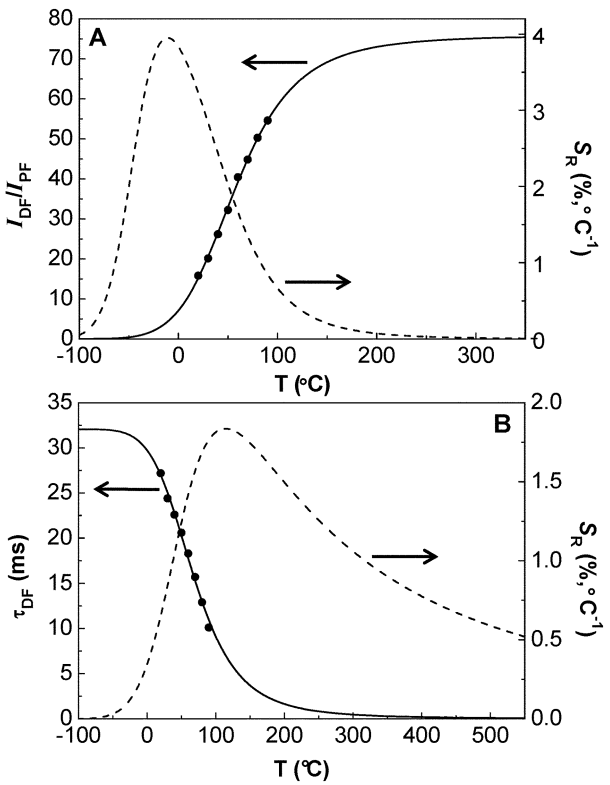

Fig. 7 (A) Experimental I_{DF}/I_{PF} values (700 nm, ●), calculated I_{DF}/I_{PF} values (—), and relative variation S_R in fluorescence intensity (---) *versus* the temperature for PS-C_{70} nanoparticles; (B) Experimental τ_{DF} values (700 nm, ●), calculated τ_{DF} values (—), and relative variation S_R in fluorescence lifetime (---) *versus* the temperature for PS-C_{70} nanoparticles.

the other hand, the Φ_F of Ru(phen)$_3$ in PAN decreases with the temperature, dropping to $\Phi_F = 0.026$ at 80 °C.[13] At this temperature the PS-C_{70} sensor has the same fluorescence quantum yield. However, while for Ru(phen)$_3$ in PAN the Φ_F decreases for higher temperatures, the Φ_F of PS-C_{70} increases (ESI,† Fig. S2), and thus the PS-C_{70} sensor outperforms Ru(phen)$_3$ in terms of quantum yield, for temperatures higher than 80 °C.

The relative temperature sensitivity (S_R) can be also calculated for the variation of the delayed fluorescence lifetime (τ_{DF}) with temperature:

$$\tau_{DF} = \left(k_G^T + Be^{\left(-\frac{\Delta E_{ST}}{RT}\right)}\right)^{-1} \quad (3)$$

where k_G^T is the nonradiative rate constant for dectivation to the ground state through intersystem crossing from T_1. In Fig. 7B we show the experimental and calculated values of τ_{DF} at 700 nm (Fig. 6), and the relative sensitivity S_R calculated from the delayed fluorescence lifetime. In this case, the temperature working range of PS-C_{70} is from 10 °C to at least 565 °C. This upper limit is just a theoretical value and is limited by the thermal stability of the material used for encapsulation of C_{70} and the matrix. The same working range can be assumed for PS-C_{70}/PAN, because it exhibits the same fluorescence intensity profile (*cf.* Fig. 3 and Fig. 5) and the delayed fluorescence lifetimes are identical (Fig. 6).

Conclusions

Using miniemulsion polymerization we were able to encapsulate pristine C_{70} in polymeric nanoparticles for the first time. The polystyrene nanoparticles containing encapsulated C_{70} (PS-C_{70}) are monodisperse and can be prepared with different diameters. These particles can be incorporated in many different materials, performing surface modification if needed.

The PS-C_{70} particles were blended with polyacrylonitrile (PAN) to prepare oxygen-impermeable films. The new material was used in a fluorescence temperature sensor, taking advantage of the strong temperature dependence of C_{70} TADF. Due to the shielding effect of PAN, it was possible to use the sensor in the presence of oxygen for a wide range of working temperatures, exceeding other known fluorescence temperature sensors. This was the first observation of TADF in materials under atmospheric oxygen concentrations. The polymeric nanoparticles developed in this work open a promising route for the use of unmodified fullerenes in materials where the fullerenes are insoluble or sparingly-soluble. These include most polymers, as well as inorganic and metallic networks.

Acknowledgements

This work was partially supported by Fundação para a Ciência e a Tecnologia (FCT, Portugal) and POCI 2010 (FEDER) within project PDCT/CTM/68451/2006. V. A. also thanks FCT for a Ph.D. grant (SFRH/BD/42322/2007). The authors thank Dr. Aleksander Fedorov from CQFM-IN for technical assistance with the picosecond lifetime decays and Prof. Dr. Emilio Palomares and Dra. Eugenia Martínez from ICIQ in Tarragona, Spain, for the TEM images.

References

1 H. W. Kroto, J. R. Heath, S. C. O'Brien, R. F. Curl and R. E. Smalley, *Nature*, 1985, **318**, 162.
2 W. Krätschmer, K. Fostiropoulos and D. R. Huffman, *Nature*, 1990, **347**, 354.
3 F. Langa and J. F. Nierengarten, *Fullerenes: Principles and Applications*, Royal Society of Chemistry, Cambridge, 2007.
4 (*a*) R. S. Ruoff, D. S. Tse, R. Malhotra and D. C. Lorents, *J. Phys. Chem.*, 1993, **97**, 3379; (*b*) N. Sivaraman, R. Dhamodaran, I. Kaliappan, T. G. Srinivasan, P. R. V. Rao and C. K. Mathews, *Fullerenes, Nanotubes, Carbon Nanostruct.*, 1994, **2**, 233.
5 C. Baleizão and M. N. Berberan-Santos, *Ann. N. Y. Acad. Sci.*, 2008, **1130**, 224.
6 (*a*) X. L. Chen and S. A. Jenekhe, *Langmuir*, 1999, **15**, 8007; (*b*) M. Akiyama, A. Ikeda, T. Shintani, Y. Doi, J. Kikuchi, T. Ogawa, K. Yogo, T. Takeya and N. Yamamoto, *Org. Biomol. Chem.*, 2008, **6**, 1015.
7 (*a*) G. Sastre, M. L. Cano, A. Corma, H. Garcia, S. Nicolopoulos, J. M. GonzalezCalbet and M. J. ValletRegi, *J. Phys. Chem. B*, 1997, **101**, 10184; (*b*) M. S. Galletero, H. Garcia and J. L. Bourdelande, *Chem. Phys. Lett.*, 2003, **370**, 829; (*c*) J. R. Herance, E. Peris, J. Vidal, J. L. Bourdelande, J. Marquet and H. Garcia, *Chem. Mater.*, 2005, **17**, 4097.
8 G. Brusatin and P. Innocenzi, *J. Sol-Gel Sci. Technol.*, 2001, **22**, 189.
9 C. Wang, Z.-X. Guo, S. Fu, W. Wu and D. Zhu, *Prog. Polym. Sci.*, 2004, **29**, 1079.
10 (*a*) I. Texier, M. N. Berberan-Santos, A. Fedorov, M. Brettreich, H. Schonberger, A. Hirsch, S. Leach and R. V. Bensasson, *J. Phys. Chem. A*, 2001, **105**, 10278; (*b*) C. Detrembleur, O. Stoilova, R. Bryaskova, A. Debuigne, A. Mouithys-Mickalad and R. Jerome, *Macromol. Rapid Commun.*, 2006, **27**, 498; (*c*) A. Hirsch, *Pure Appl. Chem.*, 2008, **80**, 571; (*d*) V. T. Lebedev, G. Torok, L. V. Vinogradova, D. N. Orlova, E. Y. Melenevskaya, V. N. G. Zgonnik and W. Treimer, *Fullerenes, Nanotubes, Carbon Nanostruct.*, 2004, **12**, 377.
11 K. Ando and H. Kawaguchi, *J. Colloid Interface Sci.*, 2005, **285**, 619.
12 (*a*) M. N. Berberan-Santos and J. M. M. Garcia, *J. Am. Chem. Soc.*, 1996, **118**, 9391; (*b*) F. A. Salazar, A. Fedorov and M. N. Berberan-Santos, *Chem. Phys. Lett.*, 1997, **271**, 361; (*c*) B. Valeur, *Molecular Fluorescence: Principles and Applications*, Wiley-VCH; Weinheim, 2002.
13 C. Baleizão, S. Nagl, S. M. Borisov, M. Schäferling, O. S. Wolfbeis and M. N. Berberan-Santos, *Chem.–Eur. J.*, 2007, **13**, 3643.
14 S. Nagl, C. Baleizão, S. M. Borisov, M. Schäferling, M. N. Berberan-Santos and O. S. Wolfbeis, *Angew. Chem., Int. Ed.*, 2007, **46**, 2317.
15 J. P. S. Farinha, J. M. G. Martinho and L. Pogliani, *J. Math. Chem.*, 1997, **21**, 131.
16 K. Landfester, *Annu. Rev. Mater. Res.*, 2006, **36**, 231.
17 (*a*) B. Tumanskii and O. Kalina, *Radical Reactions of Fullerenes and their Derivatives*, Kluwer Academic Press, Dordrecht, 2001; (*b*) T. Cao and S. E. Webber, *Macromolecules*, 1995, **28**, 3741.
18 S. Nascimento, C. Baleizão and M. N. Berberan-Santos, in *Fluorescence of Supermolecules, Polymers and Nanosystems*, ed. M. N. Berberan-Santos, Springer, Berlin, 2008, p. 151.
19 (*a*) J. P. S. Farinha, M. T. Charreyre, J. M. G. Martinho, M. A. Winnik and C. Pichot, *Langmuir*, 2001, **17**, 2617; (*b*) J. G. Spiro, J. P. S. Farinha and M. A. Winnik, *Macromolecules*, 2003, **36**, 7791; (*c*) J. P. S. Farinha, O. Vorobyova and M. A. Winnik, *Macromolecules*, 2000, **33**, 5863; (*d*) H. H. Pham, J. P. S. Farinha and M. A. Winnik, *Macromolecules*, 2000, **33**, 5850.
20 G. Liebsch, I. Klimant and O. S. Wolfbeis, *Adv. Mater.*, 1999, **11**, 1296.
21 J. Brandrup, E. H. Immergut and E. A. Grulke, *Polymer Handbook*, Wiley, New York, 1999.
22 K. T. Grattan and Z. Y. Zhang, *Fiber Optic Fluorescence Thermometry*, Chapman and Hall, London, 1995.
23 (*a*) J. N. Demas and B. A. DeGraff, *Coord. Chem. Rev.*, 2001, **211**, 317; (*b*) S. Uchiyama, A. P. de Silva and K. Iwau, *J. Chem. Educ.*, 2006, **83**, 720.
24 C. McDonagh, C. S. Burke and B. D. MacCraith, *Chem. Rev.*, 2008, **108**, 400.
25 (*a*) R. Narayanaswamy and O. S. Wolfbeis, *Optical Sensors for Industrial, Environmental and Clinical Applications*, Springer, Berlin, 2004; (*b*) F. Baldini, A. N. Chester, J. Homola and S. Martellucci, *Optical Chemical Sensors*, Springer, Dordrecht, 2006.